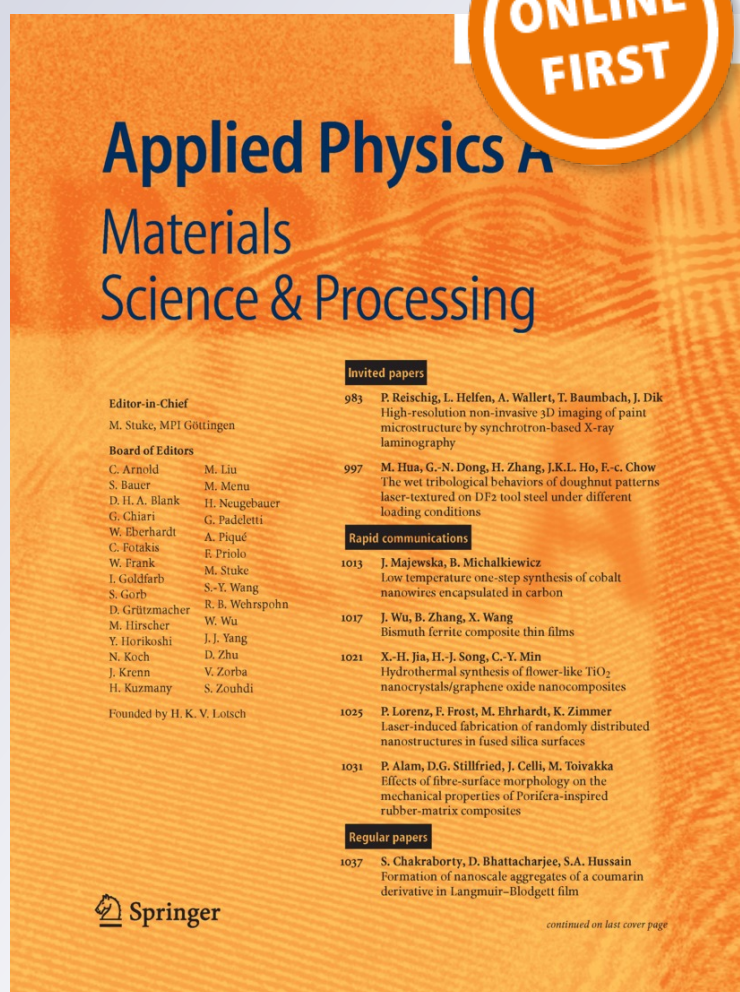# *Multilayered artifacts in the pre-Columbian metallurgy from the North of Peru*

Roberto Cesareo, Angel D. Bustamante, Julio S. Fabian, Sandra Del Pilar Zambrano, Walter Alva, Luis Z. Chero, Maria

ONLINE FIRST

Springer

Multilayered artifacts in the pre-Columbian metallurgy from the North of Peru

**Roberto Cesareo · Angel D. Bustamante · Julio S. Fabian ·
Sandra Del Pilar Zambrano · Walter Alva · Luis Z. Chero ·
Maria C. Del Carmen Espinoza · Rosendo R. Rodriguez · Marco F. Seclen ·
Fidel V. Gutierrez · Edgard B. Levano · Juan A. Gonzales · Marcia A. Rizzutto ·
Enrico Poli · Cristiane Calza · Marcelino Dos Anjos · Renato Pereira De Freitas ·
Ricardo T. Lopes · Carlos Elera · Izumi Shimada · Victor Curay · Maria G. Castillo ·
Giovanni E. Gigante · Gabriel M. Ingo · Fabio Lopes · Ulla Holmquist · David Diestra**

Abstract Three types of alloys were recognized when analyzing pre-Columbian artifacts from the North of Peru: gold, silver, and copper alloys; gilded copper and silver; silvered copper; tumbaga, i.e., copper or silver enriched on gold at the surface by depletion gilding. In this paper, a method is described to differentiate gold alloys from gilded copper and from copper–gold tumbaga, and silver alloys from silvered copper and copper–silver tumbaga. This method is based on the use of energy-dispersive X-ray fluorescence, i.e., on a sophisticated analysis of XRF-spectra carrying out an accurate determination of Cu(K_α/K_β), Ag(K_α/K_β), Au(L_α/L_β), and Au-L_α/Cu-K_α or Ag-K_α/Cu-K_α ratios. That implies a dedicated software for the quantitative determination of the area of X-ray peaks. This method was first checked by a relevant number of standard samples and then it was applied to pre-Columbian alloys from the North of Peru.

1 Introduction

On the north coast of present-day Peru (Fig. 1), between the Andes and the Pacific Ocean, several relevant cultures pros-

R. Cesareo (✉)
Dipartimento di Matematica e Fisica, Università di Sassari,
Sassari, Italy
e-mail: cesareo@uniss.it

R. Cesareo · G.M. Ingo
Istituto per lo studio dei materiali nanostrutturati,
CNR-Montelibretti, via Salaria km. 29. 5, 00015 Monterotondo,
Rome, Italy

A.D. Bustamante · J.S. Fabian · S. Del Pilar Zambrano
Universidad Nacional Mayor de San Marcos, Lima, Peru

W. Alva · L.Z. Chero · M.C. Del Carmen Espinoza ·
R.R. Rodriguez · M.F. Seclen · F.V. Gutierrez · E.B. Levano ·
J.A. Gonzales
Museo "Tumbas Reales de Sipán", Lambayeque, Peru

M.A. Rizzutto
Instituto de Fisica, Universidade de São Paulo, São Paulo, SP,
Brazil

E. Poli
Associacion cultural and Museum Enrico Poli, Lima, Peru

C. Calza · M. Dos Anjos · R. Pereira De Freitas · R.T. Lopes
COPPE, Universidade Federal do Rio de Janeiro, Rio de Janeiro,
Brazil

C. Elera · I. Shimada · V. Curay
Museo de Sicán", Ferrañafe, Peru

M.G. Castillo
Istituto Nacional de Cultura, Piura, Peru

G.E. Gigante
Dipartimento di Scienze di Base e Applicate, Sapienza Università
di Roma, Rome, Italy

F. Lopes
Universidade de Londrina, Londrina, PA, Brazil

U. Holmquist · D. Diestra
Museo Larco, Lima, Peru

pered approximately between 1200 BC and 1375 AD; the most important were: Cupisnique (1200–200 BC), Chavín (1000–200 BC),Vicús (500 BC–100 AD), Frías (400 BC–100 AD), Moche (100 AD–700 AD), Sicán (700–1375 AD), and Chimù (900–1470 AD). These cultures were interconnected and characterized by a high metallurgical ability:

Cupinisque The Cupinisque culture that reigned on the northern coast of Peru is the most ancient culture. In 2007, I. Alva discovered that people of the Cupinisque culture had built the "spider god" temple in the Lambayeque valley. I. Shimada calls Cupinisque a possible ancestor of Moche culture [1];

Chavín and Kuntur Wasi The Chavín was a civilization developed in the northern Andean highlands of Peru from about 1000 BC to 200 BC. The most known archaeological sites of the Chavín culture are Chavín de Huántar, religious center located in the Andean highlands north of Lima, built around 900 BC, and Kuntur Wasi, located in the Northern Mountain of Peru, close to Cajamarca, constructed around 1000–700 BC [3–6] and discovered by J. Tello in 1945, and then excavated by Y. Onuki [2];

Vicus The Vicús culture (200 BC–400 AD) occupied the territory of Peru's northern coastal desert from the upper Piura as far as the Macarà river and perhaps as far as the highlands of present day Ecuador. The center of the Vicús culture has been identified as Cerro Vicús (50 km east of the city of Piura), and includes the famous site of Loma Negra. Vicús metalworking was characterized by large objects manufactured by using the technique of gilding, plating, and hammering [7, 8];

Moche The Moche (or Mochica) civilization flourished in areas south of the Vicús, in the Moche and Chicama valleys, where its great ceremonial centers have been discovered, from around 100 AD to 700 AD. The Moche were known as expert metal smiths, and their ability was impressively demonstrated when Walter Alva and coworkers discovered in 1987 the "Tumbas Reales de Sipán" [9, 10]. Spectacular gold, silver, and copper funerary ornaments were excavated, and are now exposed in the namesake Museum, in Lambayeque, close to Chiclayo;

Sican (or Lambayeque) Sicán culture is the name archaeologist Izumi Shimada gave to a culture that predated the Inca in what is now the north coast of Peru between about 750–1375 BC (11). Sicán means "temple of the moon" and this culture is also referred to as Lambayeque culture, after the name of the region in Peru. The Sicán culture extended as far as present day Piura in the north and Trujillo in the south.

The following may be observed concerning previous metallurgical analyses of objects from the period ~1200 BC to ~1000 AD [12–41]:

- Various Chavín objects were analyzed [13, 14];

Fig. 1 Map of Peru and ancient north Peru civilizations (*in blue*) located around Chiclayo, Trujillo the Andes and the Ocean

- A limited number of fragments from objects from the Sipán Moche civilization were analyzed by various destructive methods [31–41]; important information was deduced from these measurements, i.e.,

  (a) Moche metalworking was based primarily upon objects made of hammered sheet metal;
  (b) Besides native gold and native gold–silver alloys (with some copper), gold and silver were already intentionally alloyed at that time;
  (c) The Moche systematically produced very low carat gold or silver alloys appearing from outside as silver or gold by depleting the surface from copper; this alloy is called *tumbaga*; the low carat alloy was burned and/or treated with acids extracted from plant juices, producing a copper oxide which was then removed mechanically, leaving the surface covered with a thin film of almost pure gold, with a gold concentration which decreases continuously with depth [32–37, 42].

Depletion gilding is a known technique which was used in many cultures worldwide, and, maybe, as early as the third millennium BC in Mesopotamia [43].

Many fragments on gold and silver (and also on silvered gold) of Moche artifacts from Loma Negra were accurately studied and analyzed by D. Schorsch [35].

Fragments from 17 Moche objects on copper, silver alloys and gold alloys from the "Museo Tumbas Reales de Sipán" have been analyzed by G. Hörz and M. Kallfass [32, 33].

S. Schlosser et al. [31] analyzed fragments from 30 objects from the Larco Museum in Lima.

A general overview of techniques suited to study gildings is presented in [44].

2 EDXRF-features and experimental set-up

EDXRF is a non-destructive and non-invasive analytical technique. When metals or alloys are analyzed, it is also a *surface analysis* in the sense that the thickness of the alloy involved in the analysis is of the order of μm to a maximum of tens of μm. The analytical results are therefore generally valid in absence of surface enrichment phenomena (patina, ions migration processes, etc.). The low penetration of fluorescent X-rays can be a problem; however, when multilayered samples are analyzed, it can also be an advantage because the surface layers are of the order of μm.

Being a surface analysis, EDXRF may be able to distinguish a gold alloy from gilded copper or tumbaga, and a silver alloy from a gilded silver, by using the internal ratio of Au, Cu, and Ag-lines, as described in Sect. 3. EDXRF analysis should also give the gold thickness value in the case of gilded copper or tumbaga (in the latter case an "equivalent thickness" may be evaluated).

In the case of copper-rich gold alloys, of gilded copper and of copper-rich silver alloys, the results of EDXRF analysis can be erroneous or affected by large uncertainties.

An energy-dispersive X-ray fluorescence (EDXRF)-equipment is mainly composed of an X-ray tube, characterized by the anode material, maximum voltage, and current, an X-ray detector, defined by energy resolution and efficiency, and a pulse height analyzer [45, 46]. Portable EDXRF equipment differs only because the X-ray source is of small size and low power, and the detector is thermoelectrically cooled and has small size Si-PIN or Si-drift.

For the first set of measurements (at the Museums of Sipán and Sicán), the portable equipment was composed of an X-ray tube (Mini-X or Eclipse II by AMPTEK-Oxford (46), which is characterized by an Ag-anode, and works at 30 kV and 100 μA maximum voltage and current, and a Si-PIN detector. For the other measurements, the portable equipment was composed of a mini X-ray tube [47] with an Ag-anode, working at 40 kV and 200 μA maximum voltage and current, and of a 123-Si-drift detector (Fig. 2) [47]. The X-ray tube output is filtered and collimated. The radiation protection problem is negligible. The specifics of employed X-ray detectors are the following:

- Si-PIN is a thermoelectrically cooled detector with about 250 μm and 7 mm² thickness and area of the Si-crystal, and a thin Be-window of 12.5 μm with about 180 eV energy resolution at 6.4 keV. This detector has an efficiency of 87 %, 24 %, and 8 % at 10, 20, and 30 keV, respectively.
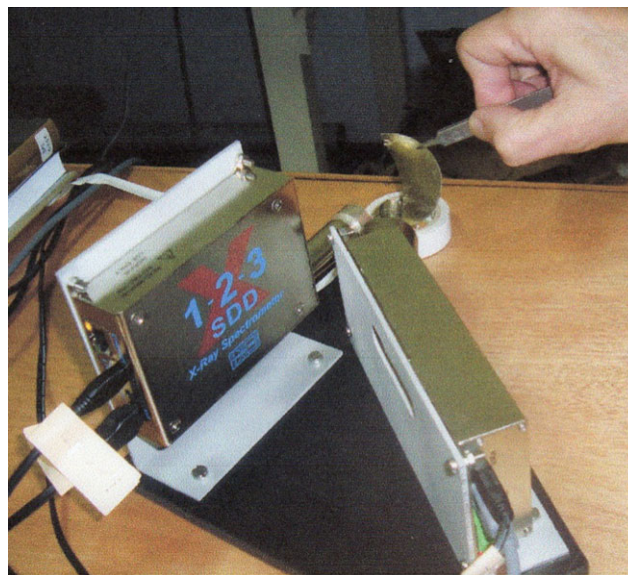

Fig. 2 EDXRF portable equipment during measurements at the Larco Museum in Lima. It is composed of a Si-drift detector (*on the left*) and an X-Ray tube (40 kV, 100 μA maximum). Electronics, including bias supply and MCA, are in the case of the 123 SDD module)

- Si-drift is a thermoelectrically cooled detector with a 500 μm, 7 mm² thickness and area of the Si-crystal, and a thin Be-window, of 12.5 μm with about 125–150 eV energy resolution at 6.4 keV. This detector has an efficiency of 97 %, 39 %, and 14 % at 10, 20, and 30 keV, respectively.

The geometrical set-up is shown in Fig. 2. The detector is put normally to the object surface; the object to be analyzed is positioned at 1.5–3 cm distance from both the X-ray tube and detector, and the irradiated area is of the order of about 10–20 mm². The measuring time ranges from about 50 s to about 200 s, depending on the sample composition and size. Standard gold alloys, containing known concentration of gold, silver and copper, and standard silver alloys, containing known concentration of silver and copper, were employed for calibration. Also calibrated Au-leafs (each Au-foil was 0.125 μm thick), silver foils, (each Ag-foil was 0.28 μm thick) and several gilded-copper samples with calibrated gilding thickness were employed.

There are, of course, many other analytical techniques for analysis of alloys, such as ICP, SEM-EDS, metallography, activation analysis, and others; all of them, however, require microsampling, which is rarely allowed. Further, the big advantage of EDXRF analysis is the possibility to analyze an object in many areas and in a short time.

3 Theoretical background

3.1 X-ray spectrum of a gold-alloy

The final result of EDXRF analysis of a sample is an X-ray spectrum containing a set of X-lines for each detectable element present in the analyzed object.

In the analysis of Au-alloys (mainly composed of Au, Cu, and Ag), of Ag-alloys (mainly composed of Ag and Cu), the following X-ray peaks are generally present: Au-*M* lines at 2.1 keV; Ag-*L* lines at 3 and 3.15 keV; Cu-*K* lines at 8 and 8.9 keV; Au-*L* lines at 8.5 (L_l), 9.7 (L_α), 10.3 (L_η), 11.44 (L_β), 13.4 ($L_{\gamma1}$), 13.8 keV ($L_{\gamma3}$); Ag-*K* lines at 22.1 and 24.9 keV.

Spurious peaks are sometimes present, due to "escape" or "sum" effect in the detector [48, 49]. The ratio of "escape peak" to the escape originating peak in an Si-detector is about 0.5–1 %, while the sum effect is one order of magnitude lower, and is, therefore, negligible.

3.2 Measurement of gilding or silvering thickness through (K_α/K_β) or (L_α/L_β) ratios or through Au-L_α/Cu-K_α, Au-L_α/Ag-K_α or Ag-K_α/Cu-K_α ratios

3.2.1 (K_α/K_β) and (L_α/L_β) ratios altered due to self-attenuation

The K_α/K_β and L_α/L_β ratios are tabulated [49–53]; they are calculated (and measured) in the approximation of infinitely thin samples, i.e., when secondary interactions in the sample are negligible. This corresponds approximately to a thickness less than 1, 0.5, 0.15, and 0.2 μm for Cu (K_α-line), Ag (K_α-line), Au (L_α-line), and Pb (L_α-line), respectively.

For an element of any thickness, self-attenuation effects must be considered, i.e., the different attenuation of K_α and K_β lines (or L_α and L_β lines) by this element.

The following theoretical equations may be then deduced for K_α/K_β or L_α/L_β ratios, due to self-attenuation [54–56]:

$$\frac{K_\alpha}{K_\beta} = \left(\frac{K_\alpha}{K_\beta}\right)_{\text{thin}} \left(\frac{\mu_0+\mu_2}{\mu_0+\mu_1}\right) \left(\frac{1-e^{-(\mu_0+\mu_1)d}}{1-e^{-(\mu_0+\mu_2)d}}\right) \quad (1)$$

$$\frac{L_\alpha}{L_\beta} = \left(\frac{L_\alpha}{L_\beta}\right)_{\text{thin}} \left(\frac{\mu_0+\mu_2}{\mu_0+\mu_1}\right) \left(\frac{1-e^{-(\mu_0+\mu_1)d}}{1-e^{-(\mu_0+\mu_2)d}}\right) \quad (2)$$

where:

- $(\frac{K_\alpha}{K_\beta})_{\text{thin}}$ and $(\frac{L_\alpha}{L_\beta})_{\text{thin}}$ represent the tabulated ratios (valid for infinitely thin samples);
- μ_0 is the linear attenuation coefficient (in cm^{-1}) of the considered element at incident energy E_0 (or mean incident energy E_0); it should be observed that this energy value is not always easy to determine when using a X-ray tube, depending on the incident X-ray beam;

- μ_1 is the linear attenuation coefficient (in cm^{-1}) of the considered element, at the energy of its K_α (or L_α) energy [57];
- μ_2 is the linear attenuation coefficient (in cm^{-1}) of the considered element, at the energy of its K_β (or L_β) radiation, respectively [57];
- d represents the thickness (in cm) of the sample.

The values of $\frac{K_\alpha}{K_\beta}$ and $\frac{L_\alpha}{L_\beta}$ ratios also depend on the X-ray spectrum from the X-ray tube, according to Eqs. (1) and (2). To limit this dependence, these ratios are normalized to 1, and may be specified as:

$$\text{Cu}\left(\frac{K_\alpha}{K_\beta}\right) = 0.795\left(\frac{1-e^{-540d}}{1-e^{-430d}}\right) \quad (3a)$$

$$\text{Ag}\left(\frac{K_\alpha}{K_\beta}\right) = 0.925\left(\frac{1-e^{-530d}}{1-e^{-490d}}\right) \quad (3b)$$

$$\text{Au}\left(\frac{L_\alpha}{L_\beta}\right) = 0.735\left(\frac{1-e^{-3900d}}{1-e^{-2860d}}\right) \quad (3c)$$

In Fig. 3, the auto-attenuation curves for $\text{Cu}(K_\alpha/K_\beta)$, $\text{Ag}(K_\alpha/K_\beta)$, and $\text{Au}(L_\alpha/L_\beta)$ are reported according to Eqs. (3a)–(3c).

It is worthwhile to observe that if the sample is not mono-elemental but, for example, an alloy, then the attenuation coefficients of Eqs. (1) and (2) should be calculated according to the alloy composition, and Eq. (3a)–(3c) may be written accordingly.

3.2.2 (K_α/K_β) and (L_α/L_β) ratios altered because of differential attenuation

When a sheet of metal, of infinite thickness, is covered by a sheet of another metal, then the ratio (K_α/K_β) or (L_α/L_β) is further so altered because of the different attenuation of the α and β-rays by the covering sheet (Fig. 4) [54–56]:

$$\frac{K_\alpha}{K_\beta} = \left(\frac{K_\alpha}{K_\beta}\right)_\infty e^{-(\mu_{1'}-\mu_{2'})d} \quad (4)$$

where

- $(K_\alpha/K_\beta)_\infty$ is the K_α/K_β ratio of the most internal metal sheet, supposedly of infinite thickness; if this sheet is not of infinite thickness, then self-attenuation effects should be considered;
- $\mu_{1'}$ is the linear attenuation coefficient of the covering sheet at the energy of K_α radiation of the element of the internal sheet;
- $\mu_{2'}$ is the linear attenuation coefficient of the covering sheet at the energy of K_β radiation of the element of the internal sheet;
- d is the thickness (in cm) of the covering sheet.

Fig. 3 Self-attenuation for copper, silver and gold: Cu(K_α/K_β), Ag(K_α/K_β) and Au(L_α/L_β) ratios versus Cu, Ag and Au thickness, respectively, normalized to 1, according to Eqs. (3a), (3b), (3c)
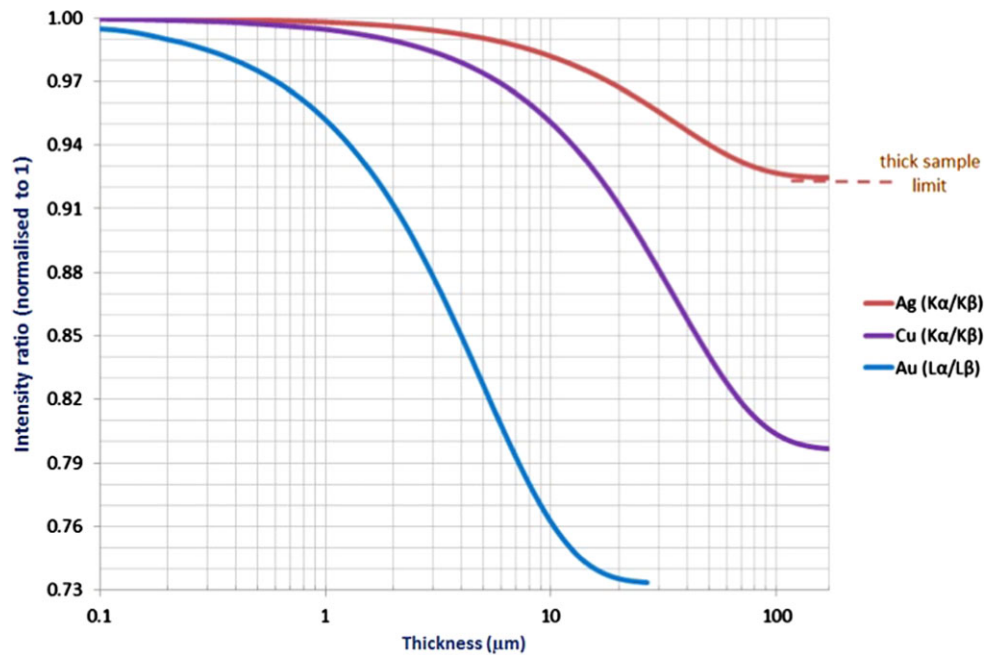
An equation similar to Eq. (4) may be deduced for the L_α/L_β ratio.

To give an example, differential attenuation of Cu-K lines by Au or by Ag is shown in Fig. 5.

Because $(\frac{K_\alpha}{K_\beta})_\infty$ ratio depends on the incident X-ray spectrum, it is convenient to normalize to 1 also Eq. (4). The following equations may be calculated for gilded Cu, silvered Cu, and gilded Ag:

$$Cu\frac{K_\alpha}{K_\beta} = e^{-930d\,(Au)} \tag{5a}$$

$$Cu\frac{K_\alpha}{K_\beta} = e^{-560d\,(Ag)} \tag{5b}$$

$$Ag\frac{K_\alpha}{K_\beta} = e^{-322d\,(Au)} \tag{5c}$$

3.2.3 Ratios (Au-L_α/Cu-K_α) versus Au thickness, and (Au-L_α/Ag-K_α) versus Ag-thickness

Another way to experimentally determine, from the X-ray spectrum, the thickness of the second element b (for example, gilding) assuming that the first element a (for example, copper) has an infinite thickness is to use of the X-ray ratio of the two elements, N_b/N_a, e.g., the ratio (Au-L_α/Cu-K_α). The generic equation is [54–56, 58]:

$$N_b/N_a = P\left(1 - e^{-[\mu(b0)+\mu(bb)]d(b)}\right)e^{[\mu(b0)+\mu(ba)]d(b)} \tag{6}$$

where

- P is a parameter to be determined according the measurements;
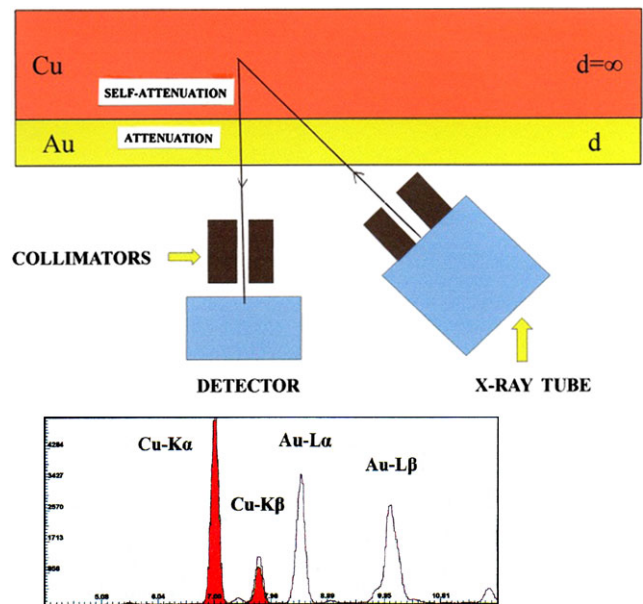
Fig. 4 Scheme of self-attenuation of Cu-K rays and attenuation of Cu-K rays by a sheet of Au (*upper figure*) and effect on the Cu K-lines. The Cu-K_β line is in both cases less attenuated than the Cu-K_α one

- μ_{b0}, μ_{ba}, and μ_{bb} are the linear attenuation coefficients of element b at incident energy E_0, and at energies of α and β lines of element b.

In the case of gilded copper, the ratio $N_b/N_a = N_{Au}/N_{Cu}$ is shown in Fig. 6.

It should be observed that an "anomalous" value for K_α/K_β or L_α/L_β ratios (lower than that with no absorber) is a certain indication of the presence of an absorbing ma-

Fig. 5 Copper X-rays attenuated by gold: Cu(K_α/K_β) ratio versus Au-thickness, normalized to 1, according to Eq. (5a); copper X-rays attenuated by silver: Cu(K_α/K_β) ratio versus Ag-thickness, normalized to 1, according to Eq. (5b); silver X-rays attenuated by gold: Ag(K_α/K_β) ratio versus Au-thickness, normalized to 1, according to Eq. (5c)
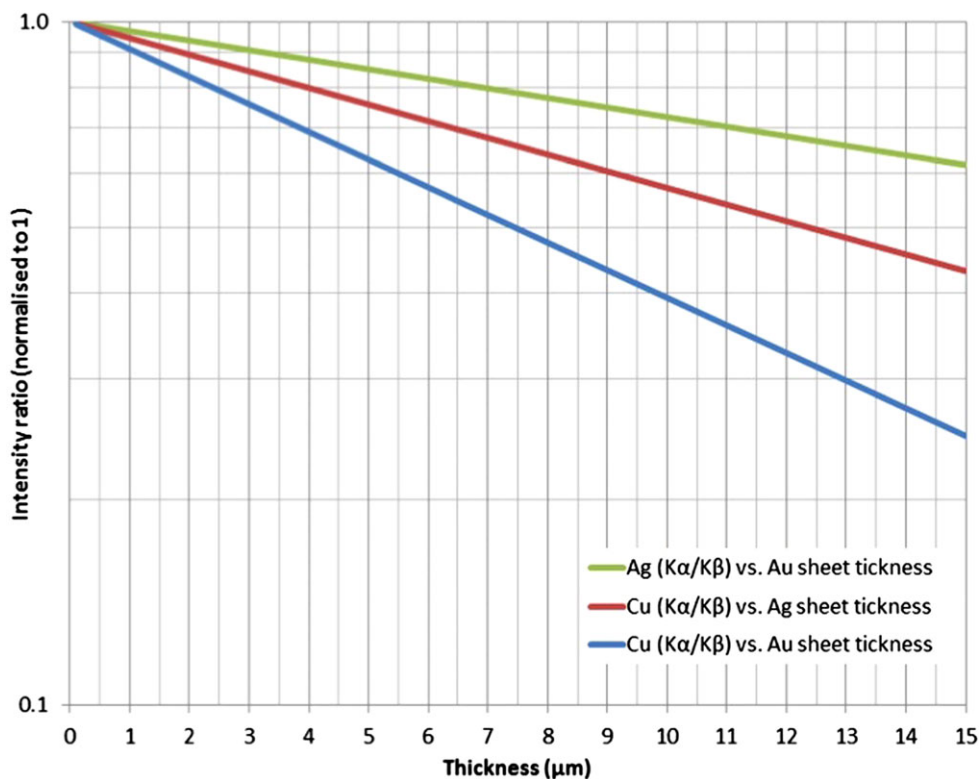
Fig. 6 Au-L_α/CuK_α ratio versus Au-thickness, according to Eq. (6)
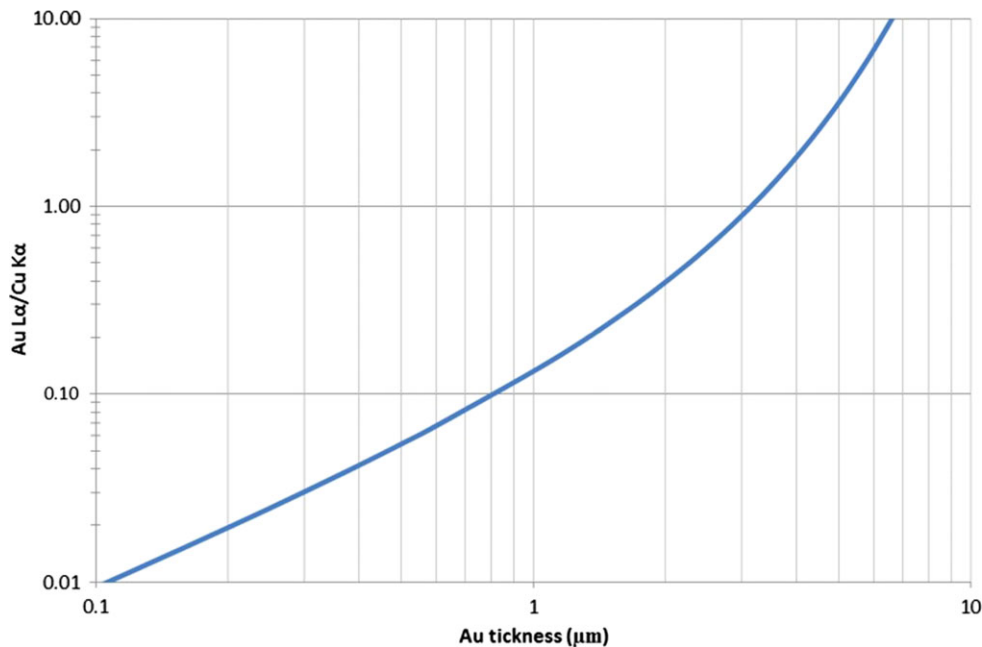
terial, while from (Au-L_α/Cu-K_α) or (Au-L_α/Ag-K_α) ratios a direct, reliable indication of the presence of an absorber is not possible. However, the latter ratios can be employed to calculate with a higher precision the thickness of an absorber, once the anomaly of K_α/K_β or L_α/L_β ratios is demonstrated.

4 From theory to practice: results for pre-Columbian alloys

4.1 Alloys from the Chavin culture

Gold, silver, and copper alloys from the Chavin culture were analyzed (1000–200 BC), located in the cultural Association

Fig. 7 Chavin vessel possibly on silver tumbaga (Museum Enrico Poli, Lima)

Fig. 8 Complex of six small heads of Chavin culture (Museo Poli, Lima), possibly on tumbaga, or, less probably, on gilded copper. X-ray tube (*top left*) and Si-drift X-ray detector (*top right*) are also visible

and Museum Enrico Poli in Lima (58), and in the Municipal Museum of Piura [60]. The analysis of single objects is discussed in details in [56].

Silver-tumbaga objects   A silver vessel of the Chavin period was analyzed, from the Museum Enrico Poli, Lima (Fig. 7). The X-ray spectrum shows the presence of copper, gold, lead (traces), and silver-lines. The internal ratio calculation of Cu, Au, and Ag is a good example of application of criteria given in Sect. 3, giving following results:

$Cu(K_\alpha/K_\beta) = 0.78 \rightarrow 2.6\ \mu m$

$Au(L_\alpha/L_\beta) = 0.91 \rightarrow 2.0\ \mu m$

$Ag(K_\alpha/K_\beta) = 0.96 \rightarrow 1.2\ \mu m$

Therefore, the vessel is composed of gilded silver, and copper is not connected to the gilding, but to silver. From these ratios it turns out that the mean thickness value is $1.9 \pm 1\ \mu m$.

The silver alloy has the following mean composition: Ag = 98%, Cu ≤ 1.5 %, Pb = 0.4 %.

Cu-tumbaga or (less probably) gilded copper objects A complex of six heads was analyzed (Fig. 8). The X-ray spectra are quite similar, and showed the presence of high quantity of copper, with lower quantities of zinc and gold, and traces of silver. The heads are, therefore, possibly on tumbaga. The following composition was determined for the Cu-body: Cu = 98.5 %, Zn = 1.5 %, Fe and Ag (traces). The ratios:

$Cu(K_\alpha/K_\beta) = 0.91 \rightarrow 1.0 \pm 0.5\ \mu m$ and

$Au(L_\alpha/L_\beta) = 0.95 \rightarrow 1.0 \pm 0.3\ \mu m$

demonstrate that the heads are composed of Cu-tumbaga or on gilded copper, and that the equivalent" gilding thickness (or gilding thickness) is approximately $1.0 \pm 0.5\ \mu m$.

The copper seems to be quite pure because the traces of silver belong to the gilding or to the Ag-anode of the X-ray tube.

4.2 ALLOYS from Vicus and Frias cultures ("Museo Municipal" of Piura and Museo Larco in Lima)

A gilded copper object   The golden feline head with sequins, teeth, and tongue from the Museum of Piura (Fig. 9) shows a sheet, just over the lips, which from the XRF-spectrum could be a Cu–Au tumbaga.

Successively, two objects from Vicús culture were analyzed in the Larco Museum (Fig. 10) [61]. Both from the altered $Cu(K_\alpha/K_\beta)$ and $Au(L_\alpha/L_\beta)$ ratios, it was deduced that the two sheets are on gilded copper. The following Au-thickness was determined: 2 μm and < 0.5 μm, respectively.

X-ray spectra show a variable Au/Cu ratio, but an almost constant (Ag/Cu) ratio = 0.01 ± 0.02, demonstrating that Ag is related to Cu, and not to Au.

4.2.1 Museo "Tumbas Reales de Sipan"

A relevant number of objects from the "Tumbas Reales de Sipán" were analyzed, on gold, gilded copper, tumbaga, silver, and copper alloys. The majority of them originate from the tomb of the "Señor de Sipán" (code S/T1); several are from the tomb of the "Sacerdote" (code S/T2); some come from the tomb of the "Viejo Señor" (S/T3), "Guerrero", and other tombs. Analyses of the single objects are shown and discussed in [56].

Gilded copper objects   Only a few analyzed objects from the "Tumbas reales de Sipán" are surely on gilded copper. They were identified by the presence of copper alone, in some analyzed areas, and also by the deteriorated surface. In many cases, it was also possible to clearly determine the Au-leaf thickness from both Cu-(K_α/K_β) and (N_{Au-L}/N_{Cu-K}) ratios.
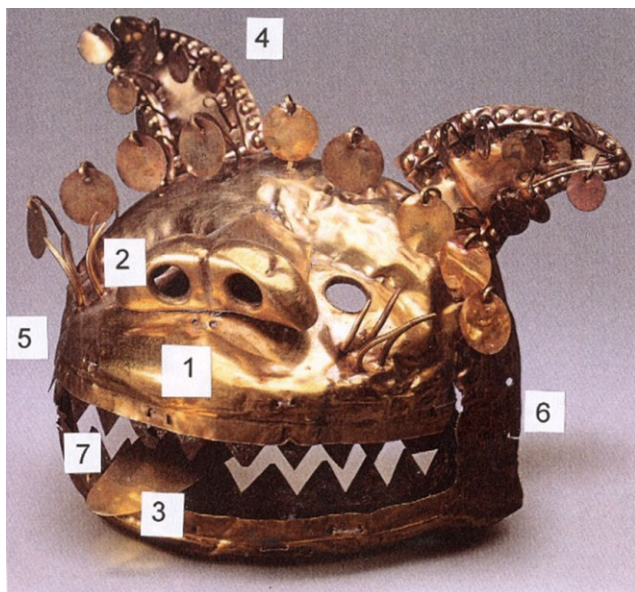
Fig. 9 Golden feline head with sequins, teeth, and tongue. The teeth are made of copper, with the following composition: Cu = 98.5 %, As = 1.5 %. Area *1*, just above the lips, is possibly on Cu–Au tumbaga

Fig. 10 Two sheets on gilded copper from the Larco Museum (ML100554 top and ML 100555)

4.3 Alloys from the Moche culture

On gilded copper there are two earrings (S/T2-O:1 and 2), where only the internal rings and the central heads are on gold, while the external sides are on gilded copper. From
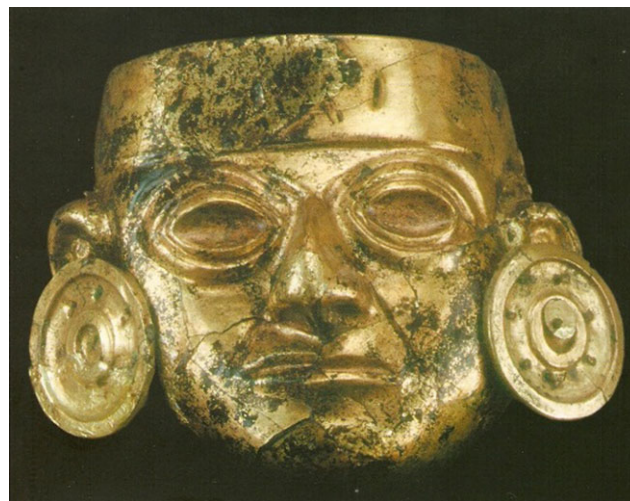

Fig. 11 Mask made of gilded copper from the tomb number 3. Areas relatively free of Cu-compounds have been analyzed. A gilding thickness of ∼0.6 μm was determined

the earring on the right, it could be deduced that the gilding thickness is 1.5 ± 0.5 μm.

A mask which is clearly on gilded copper is shown in Fig. 11. The gilding composition of this object is: Au ∼ 97.5 %, Ag ∼ 2.5 % (Cu, if present in the gilding, cannot be determined because it is present at high concentration below the gilding). The gilding thickness was measured to be ∼0.5 μm.

A thigh protector with iguanas (S/T3-Cu:71) is also possibly on gilded copper, and an Au-thickness of 0.1–0.2 μm was determined. X-ray spectra show a variable Au/Cu ratio, but an almost constant (Ag/Cu) ratio = 0.01 ± 0.02, demonstrating that Ag is related to Cu, and not to Au.

Then several sheets on gilded copper were analyzed. They are characterized by a $Cu(K_\alpha/K_\beta) = 0.89$, corresponding to a gilding thickness of 1.2 ± 0.5 μm. From the $(Au\text{-}L_\alpha/Cu\text{-}K_\alpha) = 0.06$ ratio, it turns out, however, that the value is 0.5 ± 0.1 μm.

Tumbaga objects The majority of the gold-like alloys from the "Tumbas reales de Sipán" are on tumbaga, which behaves in a similar manner as gilded-Cu for EDXRF analysis. From the X-ray spectra a "gold-equivalent" thickness[1] can be determined from $Cu\text{-}K_\alpha/K_\beta$ and from ($N_{Au\text{-}L}/N_{Cu\text{-}K}$) ratios. In Table 1, the values of the "equivalent gold-thickness" are listed, determined by both methods. It should be observed that it is difficult to give a mean composition of

---

[1]In the case of gilding (gilded copper or silver) or tumbaga (Cu–Au or Ag–Au) Au-concentration is respectively sharply or continuously decreasing from the surface; in the case of tumbaga only an "equivalent" thickness can be determined, which would be the Au-thickness producing the observed effects.

Table 1 Tumbaga gold objects (∗): "Au-equivalent" thickness, derived by the various methods described in Sect. 3

Object description and code	$N_{Au-L_\alpha}/N_{Cu-K_\alpha}$	Au-thickness (in μm)	Cu-K_α/K_β	Au-thickness (in μm)	Au-L_α/L_β	Au-thickness (in μm)
Earring with a warrior S/T1-O:2 [a] (external ring, internal circle)	1.8 ± 0.5	3.6 ± 0.2	–	–	–	–
Earring with gosling	–	–	–	–	0.9	2.4
Earring with a deer S/T1-O: 6[a] (eye of the deer, external spheres) (Fig. 12)	1 ± 1	2.9	–	–	–	–
Chin protector S/T1-0:7 (Fig. 13)	1.4 ± 0.5	3	0.86	1.4 ± 0.4	–	–
Nose decoration S/T1-0:8	0.7 ± 0.05	2.4	0.84	1.8	–	–
Nose decoration S/T1-0:9 ([b])	0.8 ± 0.1	2.7	0.78	2.6	–	–
Brain container S/T1-O:11	0.8 ± 0.2	2.7	0.84	1.8	–	–
Right eye protector S/T1-0:12 (Fig. 14)	0.75 ± 0.05	2.5	–	–	–	–
Nose protection S/T1-0:13 (Fig. 14)	0.75 ± 0.05	2.5	–	–	–	–
Convex nose protector S/T1-0:14	3.1 ± 0.3	4.4	–	–	–	–
Necklace with peanuts S/T1-O:17 (areas 86,88)	1.75 ± 0.6	3.5	0.86	1.4	–	–
Left eye protector S/T1-0:18 (Fig. 14)	0.27 ± 0.05	1.7	0.89	1.2	–	–
Tooth protection S/T1-0:23 (Fig. 14)	0.75 ± 0.05	2.5	–	–	–	–
Small rattle with a bat S/T1-O:26	0.36 ± 0.1	2.0	0.86	1.6	0.9	2.4
Crown in the form of half moon S/T1-O:28	1.4 ± 0.2	3	0.86	1.6	0.92	2
Necklace with 72 spheres S/T1-0:29	1.2 ± 0.2	3.3	–	–	0.86	3.6
Thigh protector S/T1-O:	0.85 ± 0.2	2.6	0.78	2.6	0.91	2.5
Thigh protector on Au and Ag S/T2-O: 5[a]	0.85 ± 0.05	2.6	0.79	2.4	0.95	1
Small rattle with a bat S/T3-O:8	2.2	3.8	–	–	–	–
Small rattle with a bat S/T3-O:9	2.2 ± 0.6	3.8	0.84	1.8	–	–
Big rattle with a bat S/T3-O:10	0.7 ± 0.3	2.4	0.89	1.2	0.94	1.2
Earring with an animal S/T6-O:1A (golden areas)	0.8	2.7	–	–	0.9	2.4
Earring with an animal S/T6-O:1A (eye in form of a star)	–	–	–	–	0.98	6 ± 2.5
Earring with an animal S/T6-O:1B (golden areas)	1.15	3.2	–	–	–	–
Earring with a figure S/T6-O:4A (except external decoration)	1.4	3.0	–	–	–	–
Earing with a figure S/T6-O:4A (corroded area)	–	–	–	–	0.83	4.8
Cylindrical support for earring S/T6-O:4A	1.7	3.5	–	–	–	–
Earring with a figure S/T6-O:4B (external decorations)	1.45 ± 0.9	3.1	–	–	–	–
Earring with an animal S/T6-O:6	0.8	2.7	–	–	–	–
Total mean value (μm)	0.9 ± 0.5	2.9 ± 0.6	0.84 ± 0.02	1.8 ± 0.5	0.9 ± 0.04	2.6 ± 0.8

[a]In many cases, the counting statistics was not sufficient for extracting all information

[b]The following values were obtained in a second series of measurements: Cu-$K_\alpha/K_\beta = 0.85 \pm 0.02$, Au-$L_\alpha/L_\beta = 0.91 \pm 0.04$, Au-$L$/Cu-$K = 1.03 \pm 0.06$, with a mean thickness value of 1.8 ± 1.0 μm

the tumbaga objects because it is varying with respect to depth. Under the hypothesis that at a depth higher than about 10 microns only copper will be present, it appears from the X-ray spectra that the surface composition is due to a gold–silver alloy, with the following approximate composition: Au = 82 ± 5, Ag = 18 ± 5.
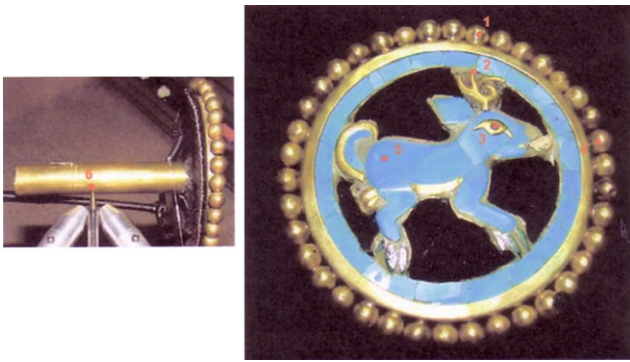
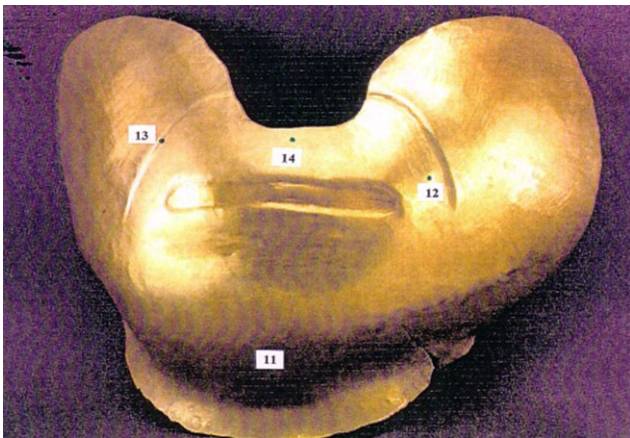**Fig. 12** Earring with a deer, with support (*on the left*). It is composed of turquoise and tumbaga

Fig. 13 Chin ornament on tumbaga. The average composition is: Au = 65 %, Cu = 26 %, Ag = 9 %. This result is compatible with the analysis of a fragment carried out by Hörz and Kallfass [9]

4.3.1 Museum "Sitio Huaca Rajada" (tomb of the "Secerdote-Guerrero") [62]

Gilded copper objects The following objects were analyzed and identified as composed of gilded copper:

- Earring. This object is very damaged, and was analyzed in five different areas where gold is still visible. The X-ray spectrum shows a high content of copper, and low quantities of Au. No Ag is present. This earring is therefore on *gilded copper*, with almost pure copper covered with a sheet of almost pure gold with a thickness, deduced from the Au-L/Cu-K ratio of about 0.4 μm, and from the $Cu(K_\alpha/K_\beta)$-ratio = 0.93 ± 0.04 of <0.7 μm.
- Feline head S/T14-Cu:42E. This object was analyzed in five different areas, and the X-ray spectra show the presence of high concentrations of Cu, and traces of Au (in three areas). Where Au is present, an approximate *gilding* thickness of 0.15 μm was determined.
- Owl crown S/T corona de buho. This object was analyzed in four different areas where gold is still visible.

Fig. 14 Protection for the eyes, nose and mouth of the "Señor de Sipán" on tumbaga. The "equivalent gilding thickness" was measured to be 2.4 μm

Fig. 15 Nose decoration on tumbaga

The X-ray spectrum shows a high content of Cu, and low quantities of Au, with a mean ratio Au-*L*/Cu-*K* = 0.05, corresponding to about 0.35 μm gilding thickness. There is no silver.

Cu–Au tumbaga objects

- Nose decoration, apparently on gold (Fig. 15). This object was analyzed in seven different areas, and showed the typical X-ray spectrum of *tumbaga*, i.e., high quantities of Cu and Au, with the Au-L/Cu-K ratio of about 2.3, corresponding to an equivalent gold thickness of about 3.5 μm, and $Au(L_\alpha/L_\beta) = 0.83 \pm 0.02$, corresponding to an equivalent thickness of 5 ± 1 μm. The $Cu(K_\alpha/K_\beta)$ could not be exactly measured because of the high background. The analysis of a black corrosion area showed no relevant difference with the other clean areas.

Fig. 16 Nose decoration on silvered copper

Fig. 17 Object in the form of a fan on gilded copper

Silvered copper objects

- Nose decoration (Fig. 16). This object was analyzed in four different areas. The X-ray spectra showed the presence of high quantities of Cu and Ag, and traces of Fe, Au, and Br.

4.4 Sican (or Lambayeque) culture

About 20 objects from the Museum of Sicán [63] and three from the Museum Larco were analyzed. The majority of them are on gilded copper, the rest are on gold, tumbaga, silver, and copper alloys. The analysis of the single objects is discussed in [56].

Gilded copper objects

- Object in the form of a fan (Fig. 17). The gilding thickness as determined from the ratios:
  $Cu(K_\alpha/K_\beta) = 0.62 \pm 0.1$, which corresponds to 5 ± 2.5 μm,
  $Au\text{-}L_\alpha/Cu\text{-}K_\alpha = 0.65$ which corresponds to 4.5 μm, and
  $Au\text{-}L_\alpha/Cu\text{-}K_\alpha = Au\text{-}L_\alpha/L_\beta = 0.85$ which corresponds 4 μm.

Several corrosion areas are present, showing a composition of about Cu = 98 %, Fe = 2 %.

- Disk (Fig. 18). The gilding thickness was determined from the ratios:
  $Cu(K_\alpha/K_\beta) = 0.6 \pm 0.05 \rightarrow 5 \pm 2$ μm,
  $Au\text{-}L_\alpha/Cu\text{-}K_\alpha = 2.9 \rightarrow 4.2$ μm.

Several corrosion areas are present, showing a mean composition of Cu = 99.5 %, As = 0.5 %.

- Second disk (MNS-149). The gilding thickness as determined from the ratios:
  $Cu(K_\alpha/K_\beta) = 0.93 \pm 0.05 \rightarrow 1 \pm 0.4$ μm,
  $Au\text{-}L_\alpha/Cu\text{-}K_\alpha = 3.0 \rightarrow 4.5$ μm.

Fig. 18 Disk on gilded copper

Several corrosion areas are present, showing a mean composition of Cu = 99.3 %, As = 0.7 %.

- Mask "las ventanas". The gilding thickness as determined from the ratios:
  $Cu(K_\alpha/K_\beta) = 0.85 \pm 0.04 \rightarrow 1.6 \pm 0.5$ μm,
  $Au\text{-}L_\alpha/Cu\text{-}K_\alpha = 0.7 \rightarrow 2.5$ μm.

Several areas are corroded, with following mean composition: Cu = 96 %, As = 4 %.

- Vase "las ventanas", highly corroded. The gilding thickness as determined from the ratios:
  $Cu(K_\alpha/K_\beta) = 0.83 \pm 0.04 \rightarrow 2$ μm,
  $Au\text{-}L_\alpha/Cu\text{-}K_\alpha = 0.4 \pm 0.05 \rightarrow 2$ μm.

Area 102 is highly corroded, showing the prevailing presence of Cu, and ratios $Au(L_\alpha/L_\beta) \sim 0.45$, corresponding to a silver thickness of about 20 μm (however, a restoration process may not be excluded). Areas 103 and 104 of the

same object show the following composition: Cu = 96 %, As = 4 %;

Cu–Au tumbaga objects Several objects from the Museum of Sicán are of uncertain composition. They could be on gilded copper or on tumbaga. In fact, the gilded copper objects are often identified because of the altered $Cu(K_\alpha/K_\beta)$-ratio, and because of the presence of highly corroded areas almost on pure copper. In other cases, the ratio $Cu(K_\alpha/K_\beta)$ is altered, but no corroded areas were detected. These objects are possibly composed of tumbaga. Among them:

- Vase. The gilding thickness, determined from the Au-L_α/ Cu-K_α = 5.1, is about 6 μm. Anomalous is an area which seems to be on silvered gold, or restored. In this area, the ratio Au-L_α/Cu-K_α = 0.05, and the ratio Au-L_α/Au-L_β-ratio = 0.5, i.e., quite anomalous.
- Vase twin of the previous one (code MS 17). The X-ray spectra of the two vases are similar, except for the absence in this vase of anomalous areas; the gilding thickness is about 6 μm. It cannot be excluded that the two vases are on gilded silver alloy (silver plus copper).
- Plumes composed of various vertical sheets (MNS-158) (Fig. 19). The "equivalent gold thickness", determined from the ratios $Cu(K_\alpha/K_\beta) = 0.73 \to 3.2 \pm 1.0$ μm

$Au(L_\alpha/L_\beta) = 0.92 \to 2$ μm, and Au-L_α/Cu-K_α = $3.4 \to 4.5$ μm. Due to the absence of corrosion areas, it cannot be excluded that this object is composed of gold.
- Sicán golden mask (Fig. 20), which is the most important object, on tumbaga.

The details of the mean surface gold thickness are summarized in the following Table 2.

5 How to differentiate gold, gilded copper, and tumbaga

As an example, and on the basis of the X-ray spectra of gold alloys, gilded copper and Cu–Au tumbaga, the following X-ray spectra are shown, corresponding to an average situation (Fig. 21).

These are average conditions. From a practical point of view, gold can be always differentiated, mainly on the basis of Au (L_α/L_β)-ratio. Gilded copper and tumbaga are not always easy to differentiate, depending on the Au-thickness, which is generally thiner in the case of gilded copper. Furthermore, ancient gilded copper objects are often damaged, and copper is clearly visible.
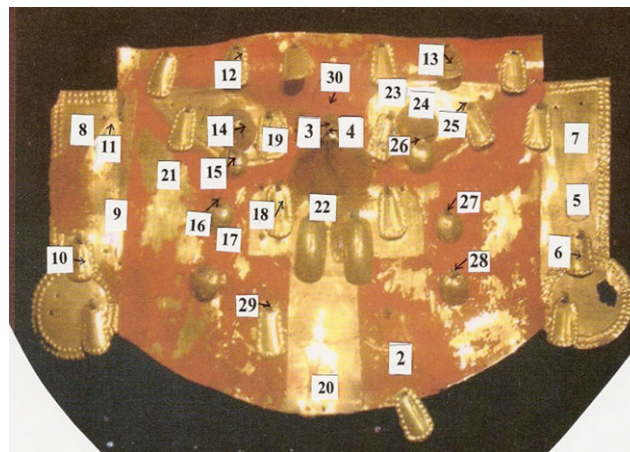

Fig. 19 Object composed of various vertical plumes (MNS-158)

Fig. 20 Mask of 35×22 cm^2 made of tumbaga, from the Museum of Sicán, and analyzed areas. The back side has the same aspect as the front side, but no areas have been analyzed. The red pigment covering the mask is cinnabar

Table 2 Mean composition of the various parts of the tumbaga mask of Fig. 20 [63]

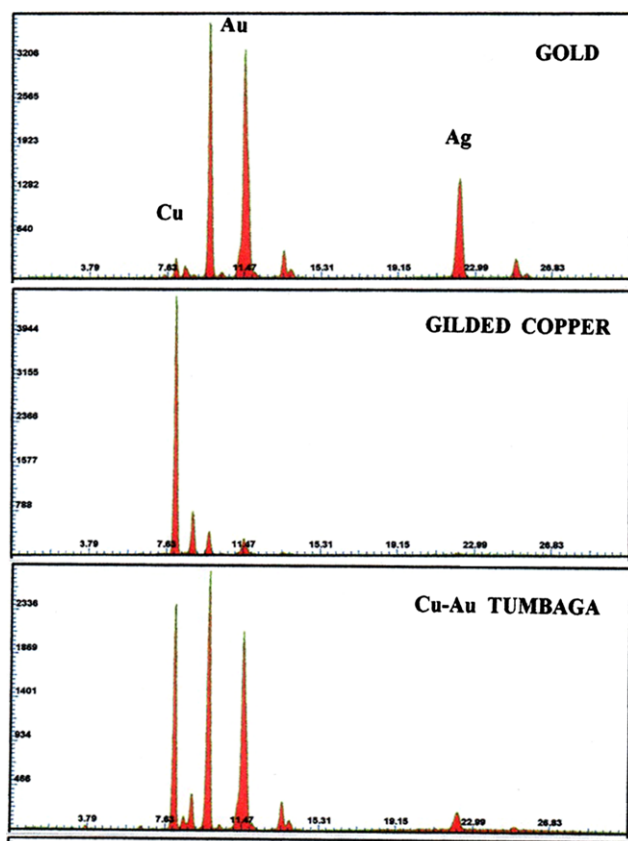| Measurement number	Au-thickness from Cu-K_α/K_β	Au-thickness from Au-L_α/Cu-K_α	Au-thickness from Au-L_α/L_β
3 (nose)	0.67 ± 0.05	4.2 ± 0.3	$0.83 \to 4.8$ μm
4 (nose)	0.73 ± 0.05	4.4 ± 0.3	$0.87 \to 3$ μm
Nose mean value (3–4)	$0.7 \pm 0.03 \to 3.8 \pm 1$ μm	$5.5 \pm 0.2 \to 5.9 \pm 1$ μm	$0.85 \to 4$ μm
8 clean areas	0.84 ± 0.03	1.4 ± 0.3	
10 pendant	0.84 ± 0.02	1.5 ± 0.3	
Mean value	$0.84 \pm 00.3 \to 1.8 \pm 0.9$ μm	$1.35 \pm 0.2 \to 2.9 \pm 0.7$ μm	$0.91 \to 2.1$ μm

Fig. 21 From the top: typical XRF-spectrum of a gold alloy, containing Ag at a concentration of about 20 % and Cu at a concentration of about 3 %; gilded copper, characterized by a high Cu-peak and low intensity Au-*L* peaks, corresponding to an Au thickness <1 μm; tumbaga, characterized by Cu-*K* and Au-*L* peaks at similar height and a low quantity of Ag. This spectrum corresponds to an "equivalent Au thickness" of about 3–4 microns

6 Conclusions on the evolution of pre-Columbian multilayers

6.1 Gilded copper

It's not easy for an object on gilded copper to be preserved during about 2000 years; there is no evidence of the use of gilded copper by the Chavin and by the Vicus-Frias; a few objects on gilded Cu from the Moche culture have survived, having a very thin Cu-layer (<1 μm). On the contrary, several objects from the Sican Museum are on gilded copper, with the characteristic Cu-layer which is relatively thick (∼5 μm) compared to Moche objects.

6.2 Cu-tumbaga

It is not clear when tumbaga was employed for the first time in Peru.

Chavin: the complex of six small heads (attributed by E. Poli to the Chavin culture) could be on tumbaga, with an equivalent Au thickness of ∼2 μm.

Vicus-Frias: among the analyzed objects of the Vicus-Frias culture, only the layer over the teeth of the feline head could be on tumbaga, with a "equivalent Au-thickness of about 1 μm".

Moche: the Moche made an extensive use of tumbaga (see Sect. 4.3); many beautiful objects were on tumbaga, with a mean equivalent Au-thickness of ∼2.5 μm.

Sican: also the Sican knew how to make tumbaga; however, their metallurgical ability was not at the level of the Moche; the mean equivalent Au-thickness is ∼3–6 μm.

6.3 Gilded silver or silver-tumbaga

A vessel (supposedly!) of the Chavin period from the Museum Poli seems to be on gilded silver (or silver-tumbaga), with an Au-thickness of about 1 μm.

6.4 Silvered copper

Only one object, the nose decoration from "Huaca Rajada", i.e., of Moche culture, is on silvered copper; the silver thickness could not be determined.

References

1. I. Shimada, *Pampa Grande and the Mochica Culture* (Univ. of Texas Press, Austin, 1994)
2. Y. Onuki, K. Inokuchi, *El Tesoro del Templo de Kuntur Wasi*, (Fondo Editorial del Congreso del Peru, Lima 2011)
3. J.C. Tello, Discovery of the Chavin culture in Peru. Am. Antiq. **9**(1), 135–160 (1943)
4. R.L. Burger, *Chavin and the Origins of Andean Civilization* (Thames and Hudson, New York, 1992)
5. R.L. Burger, Chavin de Huantar and its sphere of influence, in *Handbook of South American Archeology*, ed. by H. Silverman, W. Isbell (Springer, New York, 2008), pp. 681–706
6. http://chavin.perucultural.org.pe/kunturwasi.html
7. http://prehistoriapiura.tripod.com/vicus_frias.htm; Tiempos prehispánicos in "Breve historia de piura com/es/Cultura_Vicus"
8. http://wiki.sumaqperu.com
9. W. Alva, SIPAN: descrubrimiento e investigation. Quebecor World Perù S. A. (2004)

10. W. Alva, C.B. Donnan, The Royal Tomb of Sipán, Los Angeles Fowler Museum of cultural history; University of California (1993)

11. Sican culture in http://en.wikipedia.org/wiki/Sicanculture

12. I. Shimada, J.A. Griffin, Precious metal objects in the Middle Sicán. Sci. Am. Mag. **270**(4), 60–67 (1994)

13. S.K. Lothrop, Gold ornament of Chavin style. Am. Antiq. **16**, 226–240 (1951)

14. L. Vetter Parodi, *Gold of Ancient Peru*. Roberto Gheller Doig Ed., Lima, Peru (2006)

15. I. Shimada, J. Merkel, Copper-alloy metallurgy in ancient Peru. Sci. Am. **265**(1), 80–86 (1991)

16. I. Shimada, J.A. Griffin, Precious metal objects of the middle Sican. Sci. Am. **270**(4), 82–89 (1994)

17. J. Merkel, I. Shimada, C.P. Swann, R. Doonan, Pre-Hispanic copper alloy production at Batan Grande, Peru: interpretation of the analytical data for ore samples, in *Archaeometry of Pre-Columbian Sites and Artefacts*, ed. by D.A. Scott, P. Meyers (The Getty Conservation Institute, Santa Monica 1994), pp. 199–227

18. P. Carcedo, Metallurgia precolombian: manufactura y tecnicas en la orfebreria Sican, in *Oro del Antiguo Perù. Coleccion Arte y Tesoros del Perù. Banco de Credito del Perù en la Cultura* (1992), pp. 265–305

19. C.B. Donnan, Moche art of Peru. Pre-Columbian symbolic communication, Los Angeles, CA, Fowler Museum of Cultural History, University of California (1978)

20. J. Jones, Pre-Columbian gold, in *El Dorado, the Gold of Ancient Columbia*, New York, Center of Inter-American Relations and the American Federation of Arts (1974), pp. 21–31

21. H. Lechtman, Andean value systems and the development of prehistoric metallurgy. Technol. Cult. **25**, 1–36 (1984)

22. H. Lechtman, Traditions and styles in central Andean metalworking, in *The Beginning of the Use of the Metals and Alloys*, ed. by R. Maddin (MIT Press, Cambridge, 1988), pp. 344–378

23. J. Jones, Mochica works of art in metal: a review, in *Pre-Columbian Metallurgy of South America, Washington D.C.; Dumbarton Oaks Research Library and Collections, Trustees for Harvard University*, ed. by E.P. Benson, (1979), pp. 53–104

24. H. Lechtman, The production of copper–arsenic alloys in the Central Andes: highland ores and coastal smelters? J. Field Archaeol. **18**, 43–76 (1991)

25. P.C. Muro, I. Shimada, Behind the golden mask. Sican gold artifacts from Batan Grande, Peru, in *The Art of Precolumbian Gold. The Jan Mitchel Collection*, ed. by J. Jones (Weidenfeld and Nicolson, London, 1985), pp. 61–67

26. W. Alva, Discovering the New Word's richest tomb. Natl. Geogr. **174**(4), 510–549 (1988)

27. W. Alva, M. Fecht, P. Schauer, M. Tellenbach, *Das Fürstengrab von Sipan, Entdeckung und Restaurierung* (Verlag des Römisch-Germanischen Zentralmuseums, Mainz, 1989)

28. H. Lechtman, A pre-Columbian technique for electrochemical replacement gilding of gold and silver on objects of copper. J. Met. **31**, 154–160 (1979)

29. H. Lechtman, Pre-Columbian surface metallurgy. Sci. Am. **250**, 56–63 (1984)

30. R.L. Burger, R.B. Gordon, Early central Andean metalworking from Mina Perdida, Peru. Science **282**, 1108–1111 (1998)

31. S. Schlosser et al., Fingerprints in Gold, in *New Technologies for Archaeometry. Multidisciplinary Investigations in Palpa and Nasca, Peru*, ed. by M. Reindel, G.A. Wagner (2007), pp. 409–436

32. G. Hőrz, G. And, M. Kallfass, Pre-Columbian metalworking in Peru: ornamental and ceremonial objects from the Royal Tombs of Sipán. JOM **50**, 8–16 (1998)

33. G. Hőrz, M. Kallfass, The treasure of gold and silver artefacts from the Royal Tombs of Sipán, Peru—a study on the Moche metalworking techniques. Mater. Charact. **45**, 391–420 (2000)

34. H. Lechtman, New perspectives on Moche metallurgy: techniques of gilding copper at Loma Negra, Northern Peru. Am. Antiq. **47**(1), 3–30 (1998)

35. D. Schorsch, Silver and gold Moche artefacts from Loma Negra. Metrop. Mus. J. **33**, 109–136 (1998)

36. E.A.O. Saettone et al., Plasma clearing and analysis of archeological artefacts from Sipán. J. Appl. Phys. D **36**, 842–848 (2003)

37. H. Lechtman, Pre-Columbian surface metallurgy. Sci. Am. **250**, 38–45 (1984)

38. J.L. Ruvalcaba Sil, *X-Rays for Archaeology* (Springer Netherlands, Heidelberg, 2001), pp. 123–149

39. W. Bray, Techniques of gilding and surface enrichment in pre-Hispanic American metallurgy, in *Metal Plating and Platination*, ed. by S. La Niece, P. Craddock (Butterworth-Heinemann, Stoneham 1993), pp. 182–192

40. D.A. Scott, A review of gilding techniques in ancient South America, in *Gilded Metals: History, Technology and Conservation, Archetype*, ed. by T. Drayman-Weisser (2000), pp. 203–222

41. E. Andrade et al., IBA analysis of some precolumbian gilded copper samples. Nucl. Instrum. Methods Phys. Res. B **240**, 570–575 (2005)

42. R. Cesareo et al., Pre-Columbian alloys from the royal tombs of Sipan analyzed with a portable EDXRF equipment. Appl. Radiat. Isot. **68**, 525–528 (2010)

43. S. La Niece, Depletion gilding from 3rd millennium BC. Ur. Iraq. **57**, 41–47 (1995)

44. G.M. Ingo, E. Angelini, G. Bultrini, T. De Caro, L. Pandolfi, A. Mezzi, "Contribution of surface analytical techniques for the microchemical study of archaeological artefacts. Surf. Interface Anal. **34**, 328–336 (2002)

45. R. Cesareo, A. Brunetti, A. Castellano, M.A. Rosales, Portable equipment for X-ray fluorescence analysis, in *X-Ray Spectrometry: Recent Technological Advances*, ed. by K. Tsuji, J. Injuk, R. Van Grieken (Wiley, New York, 2004), pp. 307–341

46. R. Cesareo, *X-Ray Spectrometry in Encyclopedia for Industrial Chemistry* (Wiley-Ullmann, New York, 2010)

47. AMPTEK Inc., 6 De Angelo Drive, Bedford, MA 01730-2204, USA

48. R. Cesareo, *X-Ray Physics in: La Rivista del Nuovo Cimento* (Compositori, Bologna, 2000)

49. A. Markowicz, X-ray physics, in *Handbook on X-Ray Spectrometry: Methods and Techniques*, ed. by R. Van Grieken, A. Markowicz (M. Dekker, New York, 1992). Chap. 1

50. U. Bottigli, A. Brunetti, B. Golosio, P. Oliva, S. Stumbo, L. Vincze, P. Randaccio, P. Bleuet, A. Simionovici, A. Somogyi, Voxel-based Monte Carlo simulation of X-ray imaging and spectroscopy experiments. Spectrochim. Acta, Part B, At. Spectrosc. **59**, 1747–1754 (2004)

51. B. Ertugral et al., K_β/K_α X-ray intensity ratios for elements in the range 16–92 excited by 5.9, 59.5 and 123.6 keV photons. Radiat. Phys. Chem. **76**, 15–22 (2007)

52. W.T. Elam, B.D. Ravel, J.R. Sieber, A new atomic database for X-ray spectroscopic calculation. Radiat. Phys. Chem. **63**, 121–128 (2002)

53. T. Trojek, D. Wegrzynek, X-ray fluorescence K_α/K_β ratios for a layered specimen: comparison of measurements and Monte Carlo calculations with the MCNPX code. Nucl. Instrum. Methods Phys. Res. A **619**, 311–315 (2010)

54. R. Cesareo, A. Brunetti, Metal sheets thickness determined by EDXRF-analysis. J. X-Ray Sci. Technol. **16**(2), 119–130 (2008)

55. R. Cesareo, M.A. Rizzutto, A. Brunetti, Metal location and thickness in a multilayer sheet by measuring K- and L-ratios. Nucl. Instrum. Methods Phys. Res. B **267**(17), 2890–2896 (2009)

56. R. Cesareo, A. Bustamante, J. Fabian, W. Alva, L. Chero, M. Espinoza, R. Rodriguez, M. Seclen, F. Gutierrez, E.B. Levano, J. Gonzales, M.A. Rizzutto, E. Poli, C. Calza, M. Dos Anjos,

R.T. Lopes, G.E. Gigante, G.M. Ingo, C. Riccucci, C. Elera, I. Shimada, V. Curay, M. Castillo, F. Lopes, Evolution of pre-Columbian metallurgy from the North of Peru studied with a portable non-invasive equipment using energy-dispersive X-ray fluorescence analysis. J. Mater. Sci. Eng. B **1**, 48–81 (2011)

57. M.J. Berger, J.H. Hubbell, XCOM: photon cross sections on a personal computer. US Dept. of Commerce, NBSIR 87-3597
58. C. Fiorini, M. Gianoncelli, A. Longoni, F. Zaraga, Determination of the thickness of coatings by means of a new XRF spectrometer. X-Ray Spectrom. **31**, 92–99 (2002)
59. Museo Enrico Poli by: Associacion Civil Museo Enrico Poli, J. C. M. Lima, Peru, 2009
60. www.munipiura.gob.pe
61. www.museolarco.org
62. Huaca Rajada; www.perutours.com/index13lacasipan.html
63. R. Cesareo et al., EDXRF-analysis of a pre-Columbian funerary gold mask from the Museum of Sican, Peru. X-Ray Spectrom. **39**, 122–126 (2010)